NUCLEAR THEORY, Vol. 32 (2013)
eds. A.I. Georgieva, N. Minkov, Heron Press, Sofia

Structure of the Low-Lying Excited States in ^{99,101,103}Ru from In-Beam Fast-Timing Measurements

S. Kisyov[1], **D. Ivanova**[1], **S. Lalkovski**[1], **N. Mărginean**[2], **D. Balabanski**[3], **D. Bucurescu**[2], **Gh. Căta-Danil**[2], **I. Căta-Danil**[2], **D. Deleanu**[2], **D. Filipescu**[2], **I. Gheorghe**[2], **D. Ghiţă**[2], **T. Glodariu**[2], **R. Lica**[2], **R. Mărginean**[2], **C. Mihai**[2], **A. Negret**[2], **T. Sava**[2], **E. Stefanova**[3], **L. Stroe**[2], **R. Suvaila**[2], **S. Toma**[2], **O. Yordanov**[3], **N.V. Zamfir**[2]

[1]Faculty of Physics, "St. Kliment Ohridski" University of Sofia, Sofia, Bulgaria
[2]"Horia Hulubei" National Institute for Physics and Nuclear Engineering, Magurele, Romania
[3]Institute for Nuclear Research and Nuclear Energy, Bulgarian Academy of Science, Sofia, Bulgaria

Abstract. The neutron-deficient ^{99,101,103}Ru nuclei were studied from in-beam reaction data. The half-lives of their excited states were measured with RoSphere and preliminary results are presented. The experimental data is discussed in terms of the Rigid-Triaxial-Rotor-plus-Particle model.

1 Introduction

In the last few years a number of fast-timing experiments were performed at IFIN-HH (Romania) aiming at the structure of the low-lying excited states in the neutron-deficient odd-mass $A \approx 100$ nuclei. These studies are motivated by the large number of interesting phenomena which are observed in this mass region. In the even-even nuclei the nuclear shape may change abruptly or more smoothly depending on the number of the valence particles [1]. The shape change in the odd-mass nuclei is even more intriguing, given that different single-particle orbits have different shape-driving abilities [2].

In the focus of the present work are the low-lying states in ^{99,101,103}Ru. These nuclei have six valence holes from the $Z = 50$ shell closure (or four valence particles outside the $Z = 40$ sub-shell closure) and only a few valence neutrons outside the $N = 50$ neutron shell gap, which places them in the transitional region between the doubly magic $^{100}_{50}\mathrm{Sn}_{50}$ and the mid-shell $^{106}_{40}\mathrm{Zr}_{66}$.

2 Experimental Set Up and Data Analysis

The half-lives were measured in ^{99,101,103}Ru by using a delayed coincidence technique. The states of interest were populated in (α,nγ) reactions performed at the Tandem accelerator laboratory. Three targets, enriched in ^{96}Mo, ^{98}Mo and ^{100}Mo, where used. Their thickness was 10 mg/cm^2, 1.3 mg/cm^2 and 4 mg/cm^2, respectively. The thin targets where deposited on a 25 μm tick Pb backing in order to stop the recoils. Three different beam energies in the range of 15-18 MeV were used to maximize the yield of $^{99-103}$Ru. The typical beam intensity was in the order of 15 nA. In addition to ^{99,101,103}Ru, ^{98,100,102}Ru were also produced in the (α,2nγ) reaction channels. The γ rays, emitted in-beam, were detected by the RoSphere γ ray array consisting of 14 HPGe and 11 LaBr$_3$:Ce detectors. A detailed description of the experimental set up is given in ref. [3].

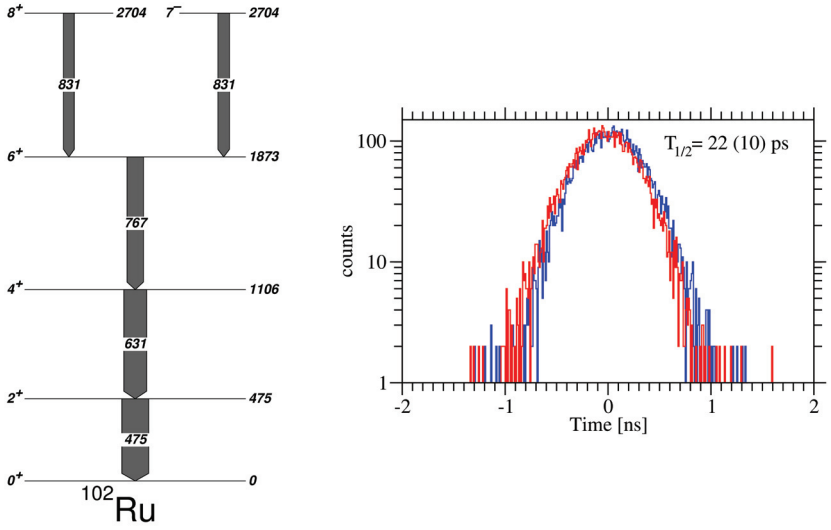

Figure 1. Partial level scheme of ^{102}Ru (left) and symmetric time spectra for the 2^+ state in ^{102}Ru (right), obtained in the present work. $T_{1/2} = 22$ (10) ps was deduced from the centroid shift method applied for the 2^+ state.

The acquisition was triggered by events where one HPGe and two LaBr$_3$:Ce detectors (2LaBr$_3$:Ce+1HPGe) OR three HPGe detectors (3HPGe) registered coincident γ rays. This logic was used to enhance the statistics in the ($E_\gamma^{LaBr} - E_\gamma^{LaBr} - \Delta T^{LaBr}$) matrices constructed from the LaBr$_3$:Ce energy and time signals, as well as in the ($E_\gamma^{HPGe} - E_\gamma^{HPGe} - E_\gamma^{HPGe}$) matrices constructed from the HPGe energy signals. The RoSphere coincidence window was set to 200 ns and the LaBr$_3$:Ce TAC ranges to 50 ns.

The experimental data were analyzed with the GASPware package [4]. Three-dimensional ($E_\gamma^{LaBr} - E_\gamma^{LaBr} - \Delta T^{LaBr}$) matrices were sorted, where for each

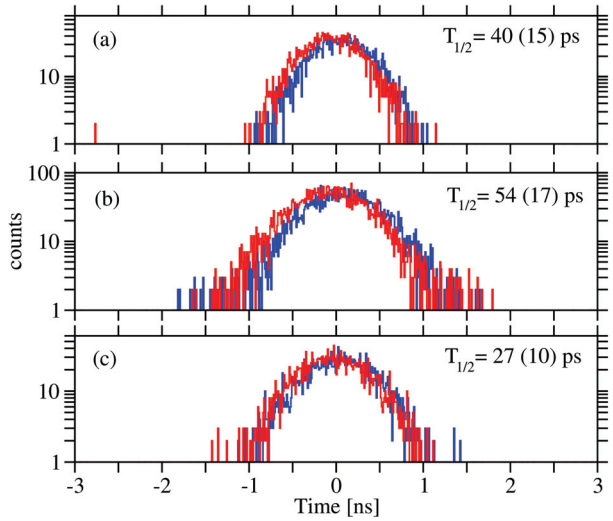

Figure 2. Time spectra for the 7/2$^+$ states in: (a) ^{99}Ru; (b) ^{101}Ru; (c) ^{103}Ru.

matrix element ($E_{\gamma_i}, E_{\gamma_j}$, ΔT_{ij}) with $\Delta T_{ij} = T_0 + (t_i - t_j)$ there is a symmetric matrix element (E_{γ_j}, E_{γ_i}, ΔT_{ji}) with $\Delta T_{ji} = T_0 - (t_i - t_j)$. Here, T_0 is an arbitrary offset and t_i and t_j are the moments in which the E_{γ_i} and E_{γ_j} were detected by the $LaBr_3$:Ce detectors. The matrices were additionally gated on γ-rays detected by any of the HPGe detectors. The data analysis, performed in the present work follows the recipes in ref. [3].

An important part of the data analysis is the evaluation of the prompt response position (PRP). Due to the walk effect, the constant fraction discriminator (CFD) time response depends on the γ-ray energy. Hence, the centroids of the prompt time distributions might appear at positions displaced with respect to the arbitrary offset T_0. This would cause an apparent half-life, which is different from the level half-life. As such, the PRP corrections has to be made. However, it should be noted that the RoSphere fine tuning, performed with fast oscilloscopes, has a practically walk free response at high γ-ray energies, i.e. $E_\gamma \sim 200$ keV or greater. In the off-line analysis, additional control on the PRP was done by using data taken with radioactive sources [3, 5] and in-beam. These procedures aim to find the walk dependence on the transition energy and to reduce its effect below the typical 25 ps guaranteed by the CFD producer [6].

Figure 1 illustrates the quality of the RoSphere timing properties. Figure 1(left) presents the partial level scheme of ^{102}Ru and Figure 1(right) shows the time spectrum for the 2$^+$ level in ^{102}Ru, obtained from the 475γ-631$\gamma(t)$ coincidences. The time spectrum is cleaned by 767 keV or 831 keV coincidence conditions imposed on the prompt distribution in the energy vs time matrix constructed from the HPGe signals. A half-life of 22 (10) ps was obtained by using

the centroid shift method, applied for the two symmetric spectra. This value is in excellent agreement with $T_{1/2} = 18.4\ (3)$ ps in ref. [7] and is about the lower limit at which the in-beam fast-timing method is still applicable, given that the Time-to-Amplitude converter resolution is about 10 ps per channel.

In more recent experiments [8], the half-life of the $15/2^-$ state in ^{103}Pd was measured by using the In-beam Fast-timing technique [3] applied with Ro-Sphere and independently obtained from a plunger experiment performed also in the same laboratory. The preliminary analysis of the plunger data shows an agreement with the fast-timing results. The deviation between the two experimental values is about 10 ps. Therefore, we adopt a systematical error of 10 ps for the Fast-timing measurements performed in the present study.

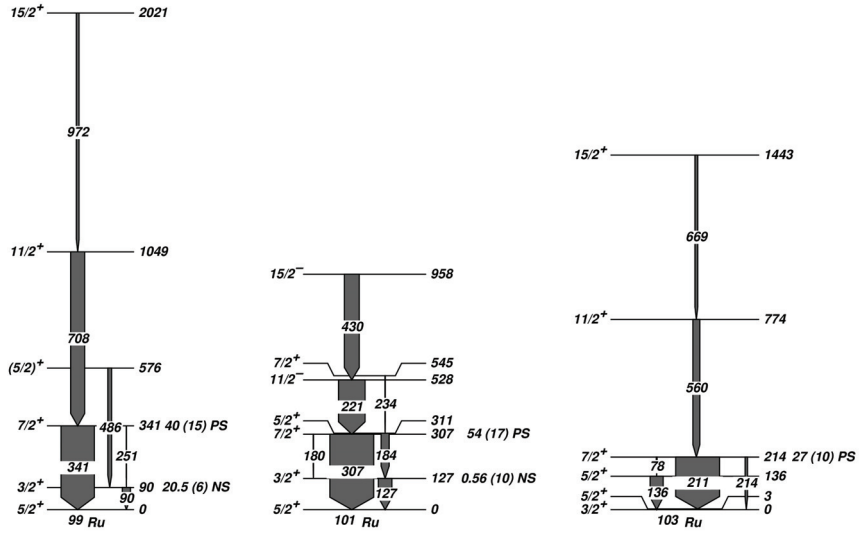

Figure 3. Partial level schemes of ^{99,101,103}Ru. The values for the half-lives are from the present work.

2.1 ^{99}Ru

The ^{99,101,103}Ru level schemes are shown in Figure 3. Prior to our study, the $3/2^+_1$ half-life in ^{99}Ru was measured in six different experiments [9] leading to $T_{1/2} = 20.47\ (9)$ ns, obtained as a weighted average of all six values. In the present study, $T_{1/2} = 20.5\ (6)$ ns was obtained from the slope of the decay curve gated on the 486 and 90 keV lines. The $3/2^+_1$ state decays via an 89.50-keV M1+E2 γ ray with a mixing ratio $\delta = -1.56\ (2)$ [9] and $\alpha = 1.50\ (3)$ which leads to $B(M1) = 0.000175\ (4)$ W.u. and $B(E2) = 50.2\ (10)$ W.u. Here, and in the calculations below, the electron conversion coefficients α are calculated with BrIcc [10].

The $7/2_1^+$ half-life is measured for the first time in the present study. It was obtained with a 972 keV gate set on the HPGe detectors and 708 keV and 341 keV gates on the $LaBr_3$:Ce detectors. Two symmetric time spectra for the $7/2_1^+$ level are shown in Figure 2 (a). $T_{1/2} = 40\ (15)$ ps was obtained from the centroid shift method. The state decays via two transitions, i.e. a 340.81 keV M1+E2 transition with $\delta = -0.020\ (5)$ and $\alpha = 0.0118\ (8)$ and a 251.0 keV E2 transition with $\alpha = 0.0492\ (8)$. The reduced transition probabilities for the 340.81 keV transition are $B(M1) = 0.014\ (6)$ W.u. and $B(E2) = 0.04\ (3)$ W.u., while for the 251.0 keV transition $B(E2) = 3.7\ (14)$ W.u.

2.2 ^{101}Ru

Prior to our study [11], the half-life of the $3/2_1^+$ state in ^{101}Ru was measured in four different experiments resulting in $T_{1/2} = 649\ (13)$ ps, obtained as a weighted average of all experimental data. The level decays via 127.226 keV M1+E2 transition with $\delta = +0.148\ (9)$ [11] and $\alpha = 0.167\ (3)$, which leads to $B(M1) = 0.0138\ (3)$ W.u. and $B(E2) = 17.2\ (21)$ W.u. $T_{1/2} = 0.56\ (10)$ ns is obtained from our study with gates set on the feeding 184 keV and the de-exciting 127 keV transitions. The time spectrum is cleaned with a gate on the 234 keV γ ray in HPGe detectors.

Prior to our study [12], the $7/2_1^+$ half-life $T_{1/2} = 53\ (14)$ ps was measured in one experiment. $T_{1/2} = 54\ (17)$ ps, deduced in the present study, is in a good agreement with the previous measurement. The time spectra were obtained with energy conditions set with the HPGe detectors on the prompt transitions feeding the $11/2^-$ isomeric state. The gates in the $LaBr_3$:Ce detectors were set on the feeding 221 keV and de-exciting 307 keV transitions. The two symmetrical spectra are presented in Figure 2 (b). The centroid shift method was used to determine the half-life. The state decays via a pure E2 179.636 keV transition with $\alpha = 0.1591\ (23)$ and a 306.857 keV M1+E2 transition with $\delta = -0.10\ (5)$ [11] and $\alpha = 0.01556\ (25)$.

The weighted average of the two measurements is $T_{1/2} = 53\ (11)$ ps and the reduced transition probability for the pure E2 transition is $B(E2) = 13.4$ W.u., while for the higher-energy mixed-multipolarity transition $B(M1) = 0.014\ (4)$ W.u. and $B(E2) = 1.4\ (14)$ W.u. were deduced.

2.3 ^{103}Ru

Prior to our study, only an upper limit of 15 ns was assigned for the $7/2_1^+$ half-life [13]. In the present work, the half-life of the $7/2_1^+$ state was measured with a gate set on the 669 keV transition in the HPGe detectors and on the feeding 560 keV and de-exciting 211 keV transitions with the $LaBr_3$:Ce detectors. The symmetric time distributions are shown in Figure 2 (c) and $T_{1/2} = 27\ (10)$ ps was deduced for this state.

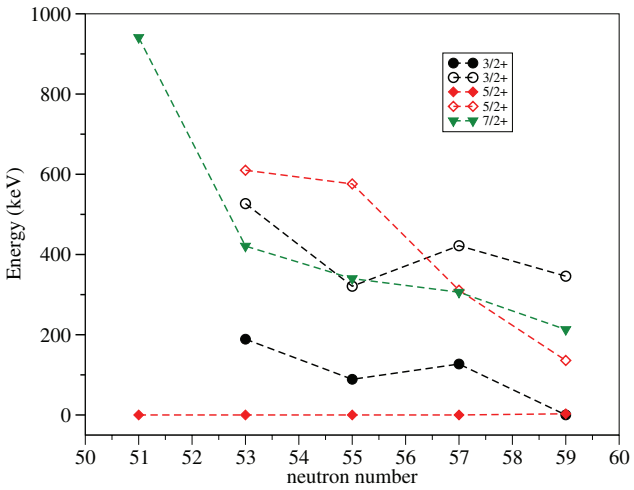

Figure 4. Evolution of the low-lying positive-parity states in the neutron-deficient Ru nuclei.

3 Discussion

The neutron-deficient ruthenium isotopes are placed in a region of the Nuclear chart where a spherical to deformed shape transition is expected. A fingerprint of such a shape change in the odd-mass ruthenium isotopes can be found in Figure 4, where low-lying ruthenium level energies are plotted as a function of the neutron number. Indeed, an abrupt change in their level schemes is observed when moving away from the semi-magic $^{94}_{44}\mathrm{Ru}_{50}$. In $^{95}\mathrm{Ru}_{51}$, which has only one valence neutron outside the closed N=50 shell, the $5/2^+$ is the ground state and the $7/2^+_1$ is at 941 keV [14]. In the gap between these two states only $1/2^+$ state, not presented in the figure, arises at 788 keV in ^{95}Ru. Already in ^{97}Ru a number of positive-parity states appear. Two $3/2^+$ states were observed at low energies, having a staggering behaviour with the neutron number increase. The $7/2^+_1$ level, which appears at approximately 1 MeV in ^{95}Ru drops in energy to about 400 keV in ^{97}Ru and then its energy smoothly decreases towards the neutron mid shell. The second $3/2^+$ state, which appears close to the ground state in $^{97-103}$Ru is correlated with the first $3/2^+$ state. The first $5/2^+$ state, which is at about 600 keV in ^{97,99}Ru drops quickly in energy and in ^{103}Ru it is at only about 100 keV above the ground state.

The contrast between the level schemes of ^{95}Ru and the heavier ruthenium nuclei, suggests that the isotopes with $N \geq 53$ exhibit a certain degree of collectivity. In order to study the collective properties of ^{99,101,103}Ru Triaxial-Rotor-plus-Particle calculations were performed. The comparison of the calculated to the experimental matrix elements will give a direct measure of the purity of the low-lying states wave functions.

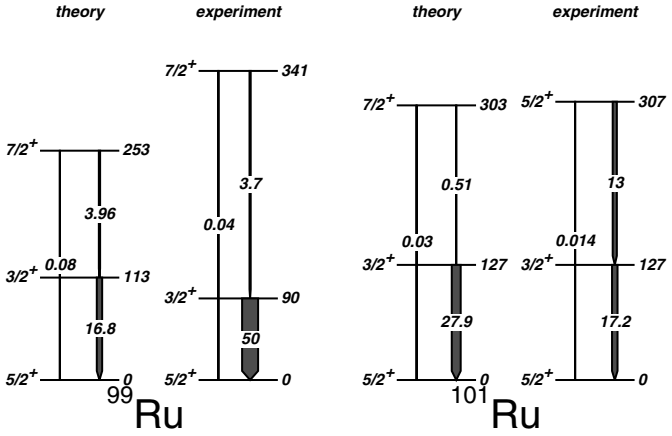

Figure 5. Rigid Triaxial Rotor model calculations for ^{99,101}Ru compared to the experimental data .

Rigid Triaxial Rotor plus Particle (RTRP) model [15] calculations were performed for the odd-mass ruthenium isotopes by using the ASYRMO code [16], which comprises three sub-codes (GAMPN, ASYRMO, PROBAMO) calculating level energies and transition probabilities.

The single-particle energies in a triaxially deformed modified harmonic oscillator potential were calculated with GAMPN. The deformation parameters ϵ_2 and ϵ_4 parameters were adopted from [17]. The parameter of triaxial deformation $\gamma = (1/3)\arcsin\sqrt{(9/8)(1-(X-1)^2/(X+1)^2)}$ is deduced from the level energy ratio $X = E_{2_2^+}/E_{2_1^+}$, calculated for the neighbouring even-even core. The standard Nilsson parameters $\kappa_4 = 0.070$ and $\mu_4 = 0.39$ and $\kappa_5 = 0.062$, $\mu_5 = 0.43$ [16, 18] were used for the fourth and fifth oscillator shell, respectively. Also, pairing parameters $GN0 = 22.0$, $GN1 = 8.0$ and $IPAIR = 5$, standard for the $Z \leq 60$ nuclei [16] were used.

The core moment-of-inertia parameter was calculated from $E_{2_1^+}$ level energy in the neighbouring even-even nuclei [19]. The particle-rotor level energies were calculated with ASYRMO in a strong coupling basis. A Coriolis attenuation parameter $\chi = 0.8$ was used. The deformation parameters were varied around the initial values in order to obtain a better fit to the experimental level energies. The final parameters, used to obtain the theoretical level schemes in Figure 5, are listed in Table 1. The transition probabilities in ^{99,101}Ru were calculated with the GAMPN code, which uses the particle-core wave functions calculated with ASYRMO. The arrow thickness in Figure 5 is proportional to the reduced transition probabilities $B(E2)$.

The calculations are consistent with the experimental data from the present experiment, suggesting that the neutron deficient ^{99,101,103}Ru nuclei are triaxially deformed at low excitation energies. These results are consistent with pre-

Table 1. Model parameters

nucleus	ϵ_2	ϵ_4	γ	E_{2+}
^{99}Ru	+0.142	-0.070	24.0	0.540
^{101}Ru	+0.167	-0.065	29.0	0.475

vious studies in the neighbouring nuclei.

4 Conclusion

The low-lying excited states in ^{99,101,103}Ru were studied from in-beam data. The half-lives were measured using fast-timing methods applied with a hybrid γ-ray array. The shortest (22 (10) ps) and the longest (20.5 (6) ns) half-lives, measured in the present study by using the same set up, cover a wide time range of three orders of magnitude. Given that the estimated systematic uncertainty is of order of 10 ps, the only constrain on the precision of the half-life measurements was the statistical uncertainty and the structure of the background in vicinity to the peaks of interest.

The new experimental data were compared with theoretical calculations within the Rigid-Triaxial-Rotor-plus-Particle model. A good overall description was achieved by using model parameters deduced from the neighbouring even-even nuclei. Therefore, ^{99,101,103}Ru are interpreted as triaxially deformed at low-energies.

Acknowledgments

This work is made as a part of the NUPNET-FATIMA Collaborations and funded by the Bulgarian Science Fund, contract numbers DMU-02/1, DNS7RP01/4, DID-05/16, and by the Bulgarian-Romanian partnership contract numbers DNTS-02/21 and 460/PNII Module III.

References

[1] R.F. Casten, *Nuclear Structure from a Simple Perspective* (Oxford Science Publishing, 2000).

[2] S.G. Nilsson and I. Ragnarsson, *Shapes and Shells in Nuclear Structure* (Cambridge University Press, 1995).

[3] N. Mărginean, *et al.*, *Eur. Phys. J. A* **46** (2010) 329-336.

[4] N. Mărginean, Private Communication (2009).

[5] J.-M. Regis, G. Pascovici, J. Jolie, M. Rudigier, *Nucl. Instrum. Methods Phys. Res., Sect. A* **A622** (2010) 83.

[6] *Model 935 Quad Constant-Fraction 200-MHz Discriminator Operating and Service Manual*

[7] D. De Frenne, *Nucl. Data Sheets* **110** (2009) 1745.

[8] D. Ivanova, *et al.*, "*Sub-nanosecond half-lives in ^{103,105}Pd from in-beam measurements*", in preparation

[9] E. Browne, J.K. Tuli, *Nucl. Data Sheets* **112** (2011) 275.

[10] T. Kibédi, T.W. Burrows, M.B. Trzhaskovskaya, P.M. Davidson, C.W. Nestor, Jr., *Nucl. Instrum. Methods* **A589** (2008) 202.

[11] J. Blachot, ENSDF for ^{101}Ru as retrieved on 9/10/2013

[12] R.B. Begzhanov, D.A. Gladyshev, K.S. Azimov, M. Narzikulov, K.T. Teshabaev, *Izv. Vyssh. Ucheb. Zaved., Fiz.* **9** (1973) 82.

[13] D. De Frenne, *Nucl. Data Sheets* **110** (2009) 2081.

[14] S. K. Basu, G. Mukherjee, A. A. Sonzogni, *Nucl. Data Sheets* **111** (2010) 2555.

[15] S.E. Larson, G. Leander, I. Ragnarson, *Nucl. Phys. A* **307** (1978) 189.

[16] P. Semmes and I. Ragnarsson, *The Particle+Triaxial Rotor Model: A User's Guide* (1992).

[17] P.Möler, J.R. Nix, W.D. Meyers, and W.J. Swiatecki, *At. Data Nucl. Data Tables* **59** (1995) 185.

[18] T. Bengtsson and I. Ragnarsson, *Nucl. Phys. A* **436** (1985) 14.

[19] NNDC data base (www.nndc.bnl.gov)